Dechlorination of *2,4*-dichlorophenoxyacetic acid by sodium carboxymethyl cellulose-stabilized Pd/Fe nanoparticles

Hongyi Zhou [a,*], Jian Han [a], Shams Ali Baig [b], Xinhua Xu [b]

[a] College of Biological and Environmental Engineering, Zhejiang University of Technology, Hangzhou 310032, People's Republic of China
[b] Department of Environmental Engineering, Zhejiang University, Hangzhou 310027, People's Republic of China

ARTICLE INFO

ABSTRACT

This paper describes the synthesis of sodium carboxymethyl cellulose (CMC)-stabilized Pd/Fe nanoparticles and their applications to the dechlorination of *2,4*-dichlorophenoxyacetic acid (*2,4*-D) under controlled laboratorial conditions. For this purpose batch mode experiments were conducted to understand the effects of CMC on the surface characteristics of Pd/Fe nanoparticles, optimum removal of *2,4*-D and other surface interactions mechanism. Our experimental results demonstrated considerable enhancements in particle stability and chemical reactivity with the addition of CMC to Pd/Fe nanoparticles. Transmission electron microscopy (TEM) analysis indicated that CMC-stabilized Pd/Fe nanoparticles were well dispersed, and nanoparticles remained in suspension for days compared to non-stabilized Pd/Fe nanoparticles precipitated within minutes. The isoelectric point (IEP) of the nanoparticles shifted from pH 6.5 to 2.5, suggesting that CMC-stabilized Pd/Fe nanoparticles were negatively charged over a wider pH range. Our batch experiments demonstrated that CMC-stabilized Pd/Fe nanoparticles ($0.6\,g\,Fe\,L^{-1}$) were able to remove much higher levels of *2,4*-D with only one intermediate *2*-chlorophenoxyacetic acid (*2*-CPA) and the final organic product phenoxyacetic acid (PA), than non-stabilized Pd/Fe nanoparticles or microsized Pd/Fe particles. The removal percentage of *2,4*-D increased from 10% to nearly 100% as the reaction pH decreased from 11.5 to 2.5. The optimal CMC/Fe mass ratio for the dechlorination of *2,4*-D was determined to be 5/1, and the removal of *2,4*-D was evidently hindered by an overdose of CMC.

© 2011 Elsevier B.V. All rights reserved.

1. Introduction

2,4-Dichlorophenoxyacetic acid (*2,4*-D) is the third most widely used herbicide in North America and the most widely used herbicide in the world [1]. However, its extensive use in agriculture has become a serious environmental concern. Due to its high solubility, *2,4*-D can be easily transferred into water and cause consequential harm to public health and the environment. LaChapelle et al. [2] labeled *2,4*-D as a potential environmental endocrine disruptor due to its ability to inhibit the ovulation of Xenopus oocytes. Therefore, the degradation of *2,4*-D has been a significant challenge worldwide.

The use of iron nanoparticles for cleaning up contaminants in soil and groundwater aquifers is one of the most promising environmental technologies. Zero-valent iron nanoparticles (nZVI) were successfully applied in hazardous waste site remediation [3,4] and contaminant reduction [5–8] owing to their small size and large surface area characteristics. However, due to their extremely high reactivity, the initially formed nanoparticles tend to either react

rapidly with surrounding media (e.g., dissolved oxygen (DO) or water) or agglomerate swiftly to form much larger particles or flocs, which leads to loss of reactivity [9].

Batch studies regarding the stabilization of the nZVI have been extensively investigated by different researchers. Schrick et al. [10] used poly (acrylic acid) (PAA) as delivery vehicles for stabilizing ZVI nanoparticles and observed an improvement of the transportability of PAA-supported nZVI in soil. Sun et al. [11] reported a new strategy for synthesizing fully dispersed and reactive nZVI with polyvinyl alcohol-co-vinylacetate-co-itaconic acid (PV3A) and confirmed that the PV3A-stabilized nZVI could effectively reduce trichloroethene (TCE). He and Zhao [9] and He et al. [12] developed a new class of nanoparticles prepared by modifying nZVI with sodium carboxymethyl cellulose (CMC), an environment-friendly and low-cost starch or food-grade cellulose. More recently, He and Zhao [13] confirmed that the size of CMC-stabilized nZVI could be manipulated by altering CMC molecular weights or CMC–Fe^{2+} molar ratio. Joo and Zhao [14] reported that the CMC-stabilized Pd/Fe nanoparticles could effectively degrade two chlorinated pesticides (lindane and atrazine) under aerobic and anaerobic conditions. Moreover, the CMC-stabilized nZVI displayed more stability and much greater reactivity than non-stabilized counterparts when used for reduction of
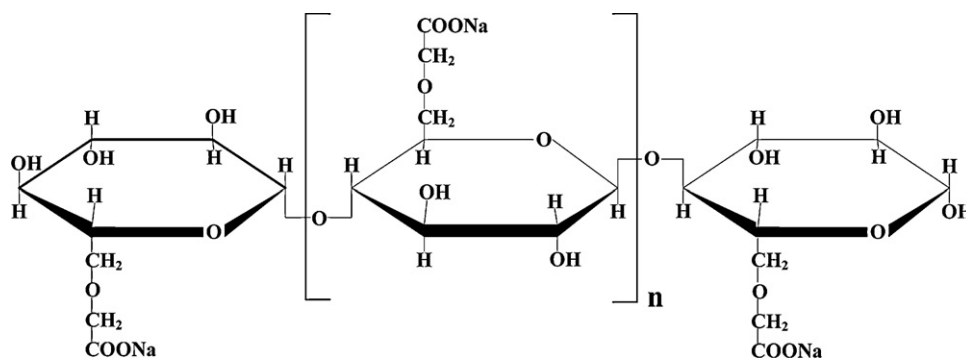

Fig. 1. Molecular structure of carboxymethyl cellulose (CMC) sodium salt.

perchlorate [15], hexahydro-1,3,5-trinitro-1,3,5-triazine (RDX) [16], nitrate [17] and hexavalent chromium [18]. He et al. [19] performed a field study during which CMC-stabilized nZVI were injected by gravity feed into a secondary source zone of PCBs and chlorinated ethenes. They observed that effective in situ degradation of chlorinated solvents could be achieved, although the mechanism of detailed transport, distribution and reaction processes of the nanoparticles were not available due to the complexity of the subsurface environment.

Main objectives of this paper were to prepare the CMC-stabilized Pd/Fe nanoparticles, and investigate the effects of CMC on surface properties of Pd/Fe nanoparticles and the removal of 2,4-D. The impact of CMC on the particle size, isoelectric point and sedimentation of Pd/Fe nanoparticles were also systematically investigated in controlled laboratorial conditions. Moreover, surface interactions mechanism was examined through ζ-potential analysis by considering pH variations associated with the ionized degree of 2,4-D and charge alterations on the surface of CMC-stabilized Pd/Fe nanoparticles. The results would provide valuable insights into the effects of CMC on the dechlorination of chlorinated contaminants in the environment by Pd/Fe nanoparticles.
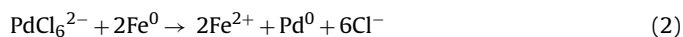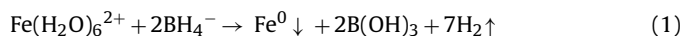
2. Materials and methods

2.1. Chemical reagents

Potassium hexachloropalladate (purity of >99%) was purchased from Sigma–Aldrich (St. Louis, MO). 2,4-D (98%), 2-chlorophenoxyacetic acid (2-CPA, 98+%), 4-chlorophenoxyacetic acid (4-CPA, 98+%) and phenoxyacetic acid (PA, 98%) were obtained from Alfa Aesar Tianjin (Tianjin, China). A water soluble sodium carboxymethyl cellulose (CMC, ionized) was purchased from Sinopharm Chemical Reagent Co. Ltd. (Shanghai, China). Ferrous sulfate (FeSO$_4$·7H$_2$O, 99.0–101.0%), Sodium borohydride (NaBH$_4$, 96%), acetone ($\geq$99.5%), sulfuric acid (H$_2$SO$_4$) (95–98%), iron power reduced (>200 mesh, >98.0%), methanol (>99.9%), and acetone of analytical grade were also used. The iron particles were pretreated by washing with acetone and sulfuric acid solution (pH = 2) that created fresh sites and made the surface more active. Deionized water was used for preparing all working and stock solutions.

2.2. Synthesis of Pd/Fe nanoparticles

Pd/Fe nanoparticles and CMC-stabilized Pd/Fe nanoparticles were synthesized according to the methods described by Wei et al. [20] and He and Zhao [9], respectively. In brief, iron nanoparticles were first synthesized by adding stoichiometric amounts of NaBH$_4$ aqueous solution to a 1 L three-necked flask containing FeSO$_4$·7H$_2$O aqueous solution and desired volumes of 10 g L^{-1} CMC solution while stirring at ambient temperature under nitrogen gas. The

palladized nZVI were then prepared by soaking the CMC-stabilized iron nanoparticles in a solution of potassium hexachloropalladate and the freshly synthesized CMC-stabilized Pd/Fe nanoparticles were subsequently used to reduce 2,4-D without additional isolation and drying. The overall process could be depicted by the following chemical reaction equations:

$$Fe(H_2O)_6{}^{2+} + 2BH_4{}^- \rightarrow Fe^0 \downarrow + 2B(OH)_3 + 7H_2 \uparrow \tag{1}$$

$$PdCl_6{}^{2-} + 2Fe^0 \rightarrow 2Fe^{2+} + Pd^0 + 6Cl^- \tag{2}$$

Cellulose is a carbohydrate consisting of a series of glucose units interconnected by an oxygen linkage (known as a beta linkage) to form a linear molecular chain structure. Cellulose can easily be modified to CMC by replacing the native CH$_2$OH group in the glucose unit with a carboxymethyl group [12]. Fig. 1 illustrates the molecular structure of CMC with n ranging from 100 to 2000. Another important reason for the selection of CMC is because of its non toxicity and biodegradability.

2.3. Reduction of 2,4-D

2,4-D stock solution (1.0 g L^{-1}) was prepared using methanol as the solvent and stored in a refrigerator at 4 °C. The batch experiments for the reduction of 2,4-D were performed in the same three-necked flask containing the CMC-stabilized Pd/Fe nanoparticles. The flask reactor was submersed in a water bath to control the temperature (25 ± 1 °C). Desired volumes of 2,4-D stock solution were then added into the flask whereas the total volume of the final water solution was 0.5 L with pH 5.0 of the resulting solution. Iron concentration used in this study was 0.6 g L^{-1} and CMC concentration (CMC/Fe, (w/w)) was accordingly varied from 2/1 to 10/1. The solution in the flask was continuously stirred at 300 rpm with a mechanical stirrer during the reaction under nitrogen flow to keep an anaerobic environment. At selected time intervals, aliquots of samples were withdrawn from the supernatant using glass syringes and then passed through 0.22 μm membrane filters for subsequent analysis. To evaluate the effect of pH variations on 2,4-D removal, all reactant solutions were adjusted to different pH values by diluted phosphoric acid (H$_3$PO$_4$) or sodium hydroxide (NaOH) prior to the initialization of the reaction. No additional pH adjustments were made during the reaction processes.

2.4. Analytical methods

2.4.1. Transmission electron microscopy (TEM)

Images of freshly synthesized Pd/Fe nanoparticles (including CMC-stabilized Pd/Fe nanoparticles) were recorded with a JEOL JEM 200CX transmission electron microscope (TEM) operated at 160 kV. The TEM samples were prepared by depositing two or three droplets of dilute ethanol solution of the nanoparticles onto a holey

carbon film. The samples were then put into a vacuumed hood till the ethanol was completely evaporated.

2.4.2. ζ-Potential and isoelectric point

ζ-Potential of the Pd/Fe nanoparticles was measured with a Zeta-Meter 3.0 (Ankersmid). This apparatus includes a microprocessor that first measures the electrophoretic mobility of colloidal particles dispersed in aqueous solutions, and then automatically calculates the zeta potential (in millivolts) using the Smoluchowski equation. The samples were immediately taken from the freshly prepared non-stabilized Pd/Fe nanoparticles and CMC-stabilized Pd/Fe solutions ($C_{Fe} = 0.2\,g\,L^{-1}$) to sealed glass tubes. The pH of the solution was adjusted by dropwise addition of 2.0 N H_2SO_4 or 2.0 N NaOH before measurement. The reliability of the ζ-potential measurements was determined by using standard deviation of the readings recorded. Each measurement of the standard deviation was $\leq 5\,mV$ and that is mechanically obtained by the instrument. Zeta potentials reported here are the average values of 10 sequential measurements.

2.4.3. Analysis of 2,4-D, 2-CPA and PA

The concentrations of 2,4-D, 2-CPA and PA were determined by a high performance liquid chromatography system (HPLC, Agilent Technologies 1200 Series) equipped with an ODS column (Hypersil, 25 μm, 4.6 mm × 150 mm) and a diode-array detector (DAD). The column temperature was set to 40 °C and the mobile phase was prepared with 0.7 L methanol and 0.3 L of 0.1% (v/v) orthophosphoric acid solution, which gave a pH value of 3.15. The flow rate of the pump was set at 0.001 L min^{-1}. The UV detection was performed at 230 nm and the detection limits for 2,4-D, 2-CPA and PA were determined to be 0.15, 0.10 and 0.10 mg L^{-1}, respectively.

3. Results and discussion

Fig. 2 presents TEM images of the Pd/Fe nanoparticles. The non-stabilized Pd/Fe nanoparticles (Fig. 2a) were largely spherical with the sizes ranging from tens to hundreds of nanometers in diameter. It can be seen that Pd/Fe nanoparticles were aggregated in chain structures due to both their magnetic properties and their tendency to remain in the most thermodynamically favorable state [21]. Most of the particles were less than 100 nm, but a few particles even had the size as large as 200 nm owing to the behavior of branched chain-like aggregates. In contrast, CMC-stabilized Pd/Fe nanoparticles shown in Fig. 2b appeared to be clearly discrete and well dispersed. Evidently, the introduction of CMC prevented aggregation of the resulting Pd/Fe nanoparticles and thus maintained the high surface area and reactivity.

Fig. 3 shows pictures of the stoppered glass tubes containing the dispersions of (a) non-stabilized Pd/Fe nanoparticles and (b) CMC-stabilized Pd/Fe nanoparticles. In settling experiments, 0.05 L of Pd/Fe nanoparticle suspensions were transferred from the flask reactor into 0.05 L tubes with flat bottoms. At the start of the experiment all test samples were uniformly black, then significant differences in the stabilizing effect of the CMC were observed. The non-stabilized Pd/Fe nanoparticles settled at the bottom of the flask in less than 3 min, while the CMC-stabilized Pd/Fe nanoparticles remained in suspension over an extended period of time (>15 days) with no noticeable sedimentation or flocculation. In addition, a small amount of Pd/Fe nanoparticles was oxidized and the color of the dispersions became yellow within 1 day. For the CMC-stabilized Pd/Fe nanoparticles, the dispersions still appeared dark even after 30 days. This observation indicated that CMC was very effective in stabilizing the Pd/Fe nanoparticles.

Enhanced stability of the CMC-stabilized Pd/Fe nanoparticles was further characterized by the increase in surface potential. In general, the extent of the electrostatic repulsion between particles
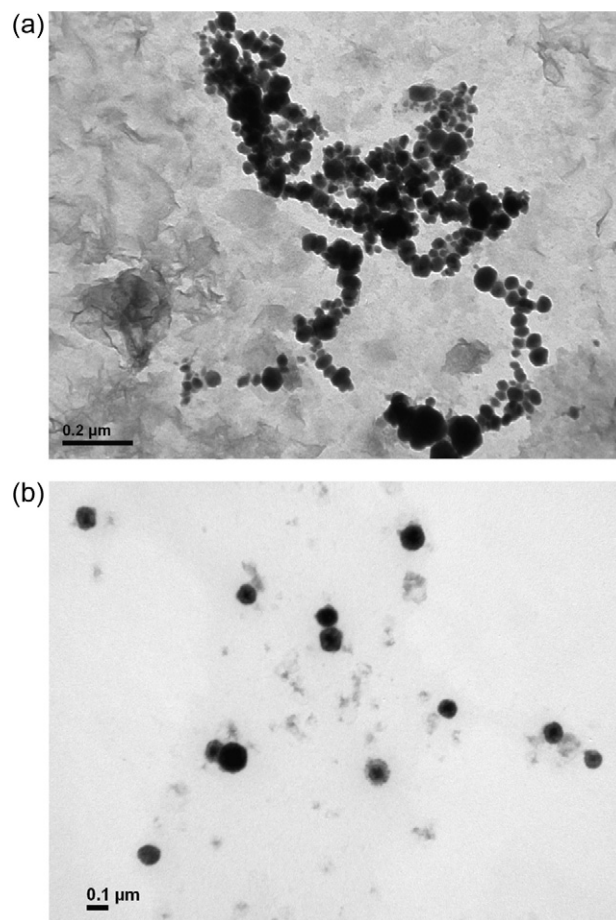

Fig. 2. TEM images of (a) non-stabilized Pd/Fe nanoparticles, and (b) CMC-stabilized Pd/Fe nanoparticles.

depends on the magnitude of the surface potential. Practically, ζ-potential is widely used as an indicator of the surface potential. A survey of existing literatures suggests that a ζ-potential of at least ±30 mV is needed to maintain a metastable suspension [22,23]. As demonstrated in Fig. 4a, Pd/Fe nanoparticles were found to maintain a surface charge of +8.84 to −14.20 mV over a pH range of 4.5–9.2. When the pH value is less than the isoelectric point (IEP) of 6.5, then Pd/Fe nanoparticles actually exhibit a positive charge. The ζ-potential becomes negative only when pH is higher than 6.5. Furthermore, under typical groundwater conditions (pH 5–8) surfaces of aquifer materials generally carry negative charges. Consequently, Pd/Fe nanoparticles with positive charges would mostly be attracted and attached to aquifer materials that led to its limited mobility in groundwater aquifer [24–26].

When the surface of Pd/Fe nanoparticles was coated with CMC, a negative charge on the particles prevailed over a much wider range. As demonstrated in Fig. 4b, CMC-stabilized Pd/Fe nanoparticles displayed negative charges at pH ≥ 2.5 by the dissociation of carboxylic acid groups on the CMC molecules. Zero-valent iron reacts with water producing hydrogen gas and hydroxide ions, which results in a typical increase of water pH. Within the pH range from 5 to 8, the ζ-potential of the CMC-coated nanoparticles was in the range of −20 mV to −30 mV. As a result, both the steric and even more substantial electrostatic repulsion caused by the large CMC molecules existed between the nanoparticles. Surfaces of soil or aquifer materials, in most cases carry negative charges and CMC-stabilized Pd/Fe nanoparticles also display negative charges. Electrostatic repulsion generated between them then should result in an enhancement of mobility [12].
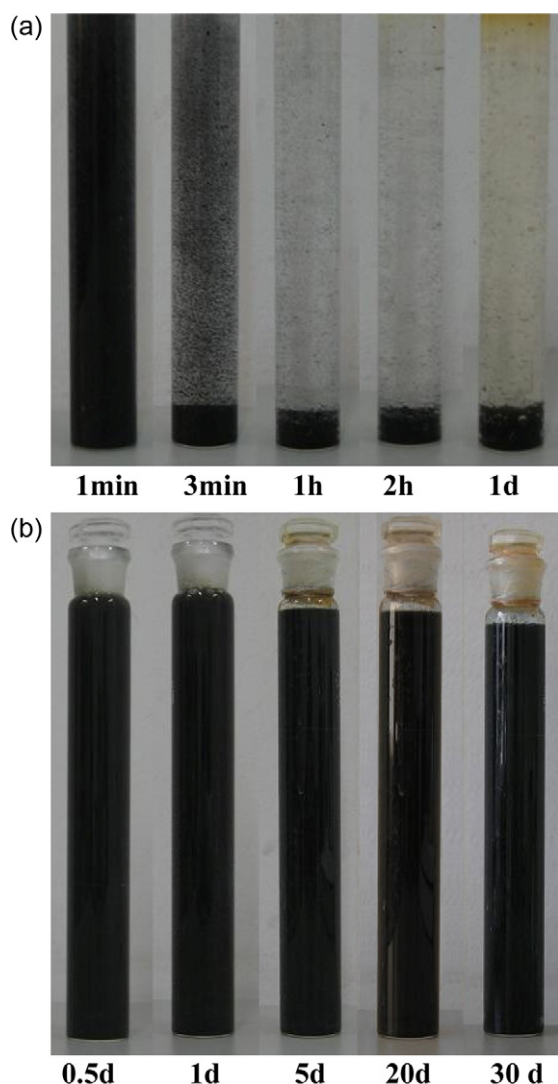
Fig. 3. Sedimentation experiments with (a) non-stabilized Pd/Fe nanoparticles, and (b) CMC-stabilized Pd/Fe nanoparticles.

Fig. 5 shows the comparison of different systems (microsized Pd/Fe, non-stabilized Pd/Fe nanoparticles and CMC-stabilized Pd/Fe nanoparticles) for the dechlorination of 2,4-D. The batch reactors contained the same initial concentration of 2,4-D ($C_0 = 10\,mg\,L^{-1}$), same concentration of iron ($0.6\,g\,L^{-1}$) and same palladium to iron ratio (0.8% (w/w)). Control conducted without palladium nor iron showed that 2,4-D was stable in water (Fig. 5). As no 2,4-D decrease was observed in a control batch reactor containing around $3\,g\,L^{-1}$ CMC (Fig. 5), it could also be deduced that sorption or partitioning of 2,4-D to CMC was negligible. The removal of 2,4-D was achieved up to 97%, 70% and 48% for CMC-stabilized Pd/Fe nanoparticles, non-stabilized Pd/Fe nanoparticles and microsized Pd/Fe particles within 180 min, respectively. The higher reactivity observed with the CMC-stabilized Pd/Fe system may be explained by the smaller size and hence higher surface area of particles.

Fig. 6 shows the time course of 2,4-D ($C_0 = 12\,mg\,L^{-1}$) dechlorination using CMC-stabilized Pd/Fe nanoparticles (CMC/Fe = 2/1 (w/w), $C_{Fe} = 1.0\,g\,L^{-1}$, Pd/Fe = 1/100 (w/w)). 2,4-D was first adsorbed [27–30] by the nanoparticles then reduced to 2-chlorophenoxyacetic acid (2-CPA), and later quickly converted to phenoxyacetic acid (PA). PA was the sole final organic product and no other chlorinated intermediate products were detected.
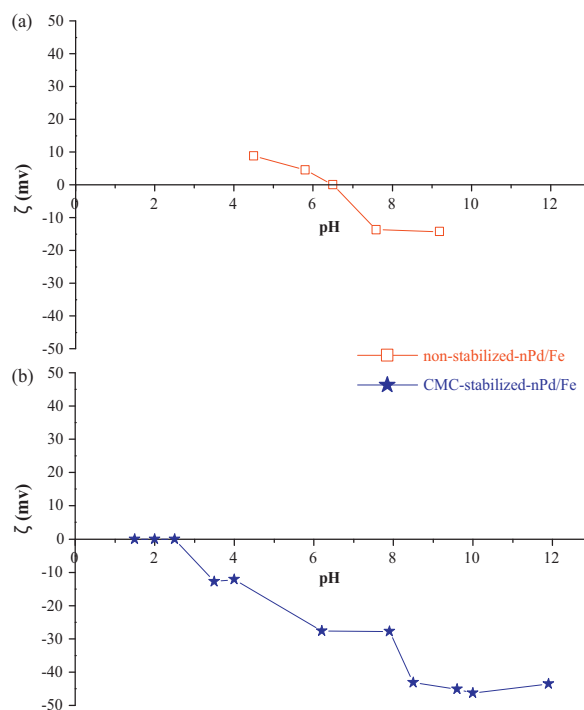

Fig. 4. Zeta (ζ)-potential as a function of solution pH: (a) non-stabilized Pd/Fe nanoparticles, and (b) CMC-stabilized Pd/Fe nanoparticles. $C_{Fe} = 0.2\,g\,L^{-1}$, Pd/Fe = 0.8/100 (w/w).

The concentration of 2,4-D ($C_0 = 12\,mg\,L^{-1}$) decreased rapidly and the removal percentage reached 66% in 30 min, and 81% in 180 min for CMC-stabilized Pd/Fe nanoparticles. The concentration of 2-CPA remained at low levels during the whole reaction period with the maximum concentration being 0.0022 mM (0.40 mg L^{-1}, 4% of the original carbon) after 15 min. PA was detected as the final organic product of the dechlorination reaction. The fast disappearance of 2,4-D during the first 5 min of reaction was attributed to sorption of the molecule on Pd/Fe nanoparticles, as supported by the delayed formation of PA. The carbon mass balances were in the range of 73–81%, so approximately 19–27% carbon mass losses were observed. A small fraction of organic compounds adsorbed or covered by surface passivating layers is most likely due to the
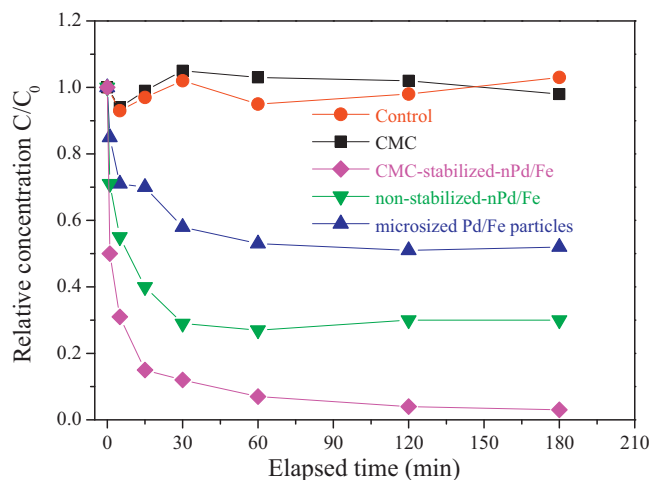

Fig. 5. Dechlorination of 2,4-dichlorophenoxyacetic acid (2,4-D) by microsized Pd/Fe particles, non-stabilized Pd/Fe nanoparticles and CMC-stabilized Pd/Fe nanoparticles ($T = 25\,°C$, $C_{2,4-D0} = 10\,mg\,L^{-1}$, $C_{Fe} = 0.6\,g\,L^{-1}$, CMC/Fe = 5/1 (w/w), Pd/Fe = 0.8/100 (w/w), stirring at 300 rpm).

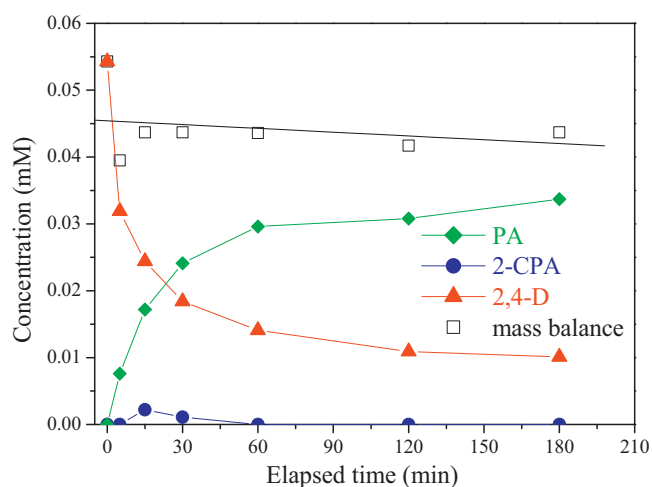**Fig. 6.** Dechlorination of *2,4*-D by CMC-stabilized Pd/Fe nanoparticles ($T = 25\,^\circ$C, $C_{Fe} = 1.0\,g\,L^{-1}$, $C_{2,4-D0} = 12\,mg\,L^{-1}$, CMC/Fe = 2/1(w/w), Pd/Fe = 1/100 (w/w), stirring at 300 rpm).

Fig. 8. Removal of *2,4*-D using CMC-stabilized Pd/Fe nanoparticles at various CMC/Fe mass ratios ($T = 25\,^\circ$C, $C_{Fe} = 0.6\,g\,L^{-1}$, $C_{2,4-D0} = 10\,mg\,L^{-1}$, Pd/Fe = 0.8/100 (w/w), stirring at 300 rpm).

fact that metal hydroxides precipitated on the surface of iron. The non-detected fraction of organics may be associated with the high surface area of Pd/Fe nanoparticles, which appear to serve as non-reactive sorption sites for organics [31].

It is apparent that almost all *2,4*-D were first transformed into *2*-CPA rather than *4*-chlorophenoxyacetic acid (*4*-CPA) and then reduced to PA during the whole degradation process. *2*-CPA was transiently formed before the formation of PA as the sole final organic product. The selective cleavage of the para C–Cl bond during the hydrodechlorination process was likely due to the steric hindrance of the –OCH$_2$COOH group. Then the chlorine atom of *2*-CPA is replaced by hydrogen and PA is formed. The overall dechlorination reaction process can be represented as:
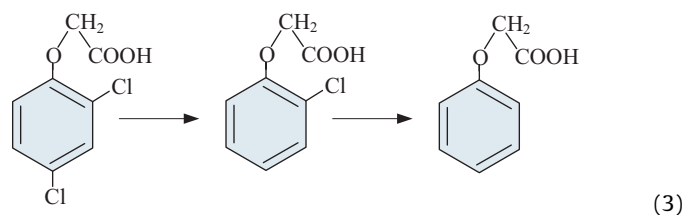

$$(3)$$

Fig. 7 shows the effect of initial pH values on the removal of *2,4*-D by CMC-stabilized Pd/Fe nanoparticles. The removal percentages of
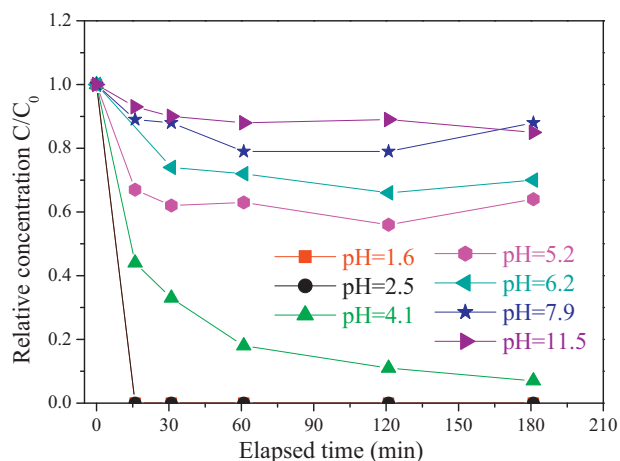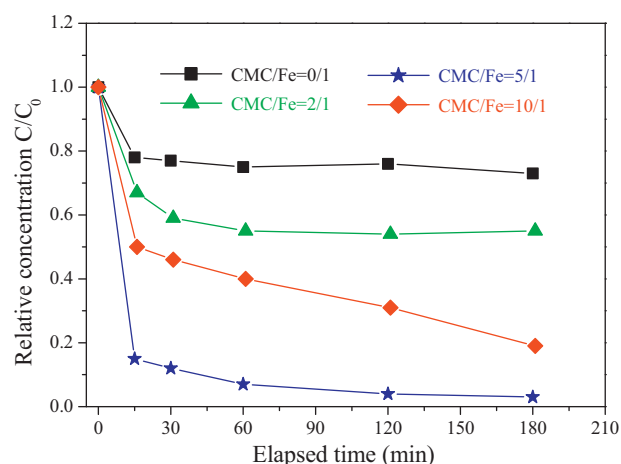

Fig. 7. Effect of initial pH values ($T = 25\,^\circ$C, $C_{Fe} = 0.6\,g\,L^{-1}$, $C_{2,4-D0} = 10\,mg\,L^{-1}$, CMC/Fe = 5/1(w/w), Pd/Fe = 0.8/100 (w/w), stirring at 300 rpm).

2,4-D dropped when initial pH values increased. When the solution pH value was 2.5, the removal percentage of *2,4*-D reached nearly 100% within minutes. However, the removal percentage of *2,4*-D dropped to ~10–15% in 180 min if pH values were adjusted to 7.9 or 11.5. Low pH (acidic) favors the corrosion of iron surface and then it provides more active sites available for reaction. At higher pH values (alkaline), oxide and hydroxide coatings will develop and thus hinder *2,4*-D access to the iron surface [32].

In addition, the removal percentages of *2,4*-D were found to be consistent with the ζ-potential. Clark et al. [27] concluded that adsorption of zero-valent iron played an important role in degrading perchloroethylene (PCE). The contaminants were first adsorbed to the surface of zero-valent iron and then catalytic reduction occurred. *2,4*-D is a phenoxyacetic acid herbicide, which has a pK_a of 2.64. If the solution pH is above the pK_a value, the concentration of the ionized *2,4*-D is greater than the concentration of *2,4*-D, which means that the ionized *2,4*-D is dominant and the solution of *2,4*-D carries negative charges. As shown in Fig. 4b, the ζ-potential of CMC-stabilized nPd/Fe was in the range of 0 mV to -50 mV in the tested pH range. At higher pH values (>4.1) low reactivity could also be due to large electrostatic repulsions between the negatively charged *2,4*-D and the negative surface of CMC-stabilized Pd/Fe nanoparticles. At low pH values (≤ 4.1), the reactivity increased because of declined electrostatic repulsion. When pH value ≤ 2.5, ζ-potential significantly increased to 0 mV and *2,4*-D could not be detected during the initial stage of the chemical reaction. It was presumed that *2,4*-D was easily adsorbed on surface of CMC-stabilized Pd/Fe nanoparticles and then quickly reduced. Therefore, the pH value is very important in reductive dechlorination of chlorinated organic acids using ZVI [33].

Fig. 8 shows the removal of *2,4*-D by CMC-stabilized Pd/Fe nanoparticles as the CMC-to-Fe mass ratio varied. It is clear that the removal percentage of *2,4*-D increased from 27% to 97% in 180 min as the CMC-to-Fe mass ratio increased from 0/1 to 5/1 (i.e. CMC was increased from 0 to 3.0 g L^{-1} for a fixed ZVI concentration of 0.6 g L^{-1}). When the CMC-to-Fe mass ratio was further increased from 5/1 to 10/1, the removal of *2,4*-D was evidently hindered, especially at the early stage of the reactions. Compared to non-stabilized Pd/Fe nanoparticles, CMC-stabilized nanoparticles displayed much enhanced reactivity, suggesting that CMC inhibited the aggregation of Pd/Fe nanoparticles and hence maintained their high reactivity. However, excessive CMC coating on the Pd/Fe nanoparticles actually reduced the reactivity of the nanoparticles as CMC might occupy the surface active sites as a result of the formation of a more

compact surface coating. Obviously, there should be an optimum CMC-to-Fe ratio, where the reactivity is maximized. Several recent published findings also confirmed this phenomenon. For example, Saleh et al. [34] reported that the reactivity of ZVI nanoparticles was reduced due to surface coating with surfactants and copolymers. He and Zhao [35] reported that higher CMC-to-Fe molar ratio lowered the dechlorination rate of trichloroethene (TCE). Furthermore, with an increasing CMC, the operation would become harder and more complex. Considering the reactivity and other factors, CMC-to-Fe mass ratio (5/1) was more appropriate.

4. Conclusions

We concluded from this study regarding the synthesis of CMC-stabilized Pd/Fe nanoparticles and the effects of CMC on *2,4*-D dechlorination. Unlike non-stabilized Pd/Fe nanoparticles that precipitated in aqueous solutions within minutes, CMC-stabilized counterparts were well dispersed and could remain in suspension for days. The addition of CMC shifted the isoelectric point of Pd/Fe nanoparticles from pH 6.5 to 2.5 and that enabled the formation of negatively charged substances over a wider pH range. CMC-stabilized Pd/Fe nanoparticles were able to effectively remove *2,4*-D as compared to non-stabilized Pd/Fe nanoparticles and microsized Pd/Fe particles. *2,4*-D was first adsorbed by the nanoparticles then reduced to *2*-CPA, and eventually converted to PA during the whole degradation process. In addition, the reaction pH and CMC-to-Fe mass ratio (CMC/Fe) significantly affected the *2,4*-D reduction. The removal percentage of *2,4*-D reached nearly 100% and 97% as the optimal reaction pH and CMC/Fe mass ratio were 2.5 and 5/1, respectively. CMC-stabilized Pd/Fe nanoparticles could be utilized in wastewater treatment. It is also feasible that this approach should be applied for treating the contamination in soil due to its enhancement in potential mobility. However, the requirement of acid pH (2.5) for the method to be efficient is a drawback for its in situ application in soil where pH values are rarely so low.

References

[1] C. Badellino, C.A. Rodrigues, R. Bertazzoli, Oxidation of pesticides by in situ electrogenerated hydrogen peroxide: study for the degradation of *2,4*-dichlorophenoxyacetic acid, J. Hazard. Mater. 137 (2006) 856–864.
[2] A.M. LaChapelle, M.L. Ruygrok, M. Toomer, J.J. Oost, M.L. Monnie, J.A. Swenson, A.A. Compton, B. Stebbins-Boaz, The hormonal herbicide, *2,4*-dichlorophenoxyacetic acid, inhibits xenopus oocyte maturation by targeting translational and post-translational mechanisms, Reprod. Toxicol. 23 (2007) 20–31.
[3] D.W. Elliott, W.X. Zhang, Field assessment of nanoscale bimetallic particles for groundwater treatment, Environ. Sci. Technol. 35 (2001) 4922–4926.
[4] J. Quinn, C. Geiger, C. Clausen, K. Brooks, C. Coon, S. O'Hara, T. Krug, D. Major, W.S. Yoon, A. Gavaskar, T. Holdsworth, Field demonstration of DNAPL dehalogenation using emulsified zero-valent iron, Environ. Sci. Technol. 39 (2005) 1309–1318.
[5] W.X. Zhang, Nanoscale iron particles for environmental remediation: An overview, J. Nanopart. Res. 5 (2003) 323–332.
[6] M.O. Nutt, J.B. Hughes, M.S. Wong, Designing Pd-on-Au bimetallic nanoparticle catalysts for trichloroethene hydrodechlorination, Environ. Sci. Technol. 39 (2005) 1346–1353.
[7] J.S. Cao, D. Elliott, W.X. Zhang, Perchlorate reduction by nanoscale iron particles, J. Nanopart. Res. 7 (2005) 499–506.
[8] S.R. Kanel, B. Manning, L. Charlet, H.C. Choi, Removal of arsenic (III) from groundwater by nanoscale zero-valent iron, Environ. Sci. Technol. 39 (2005) 1291–1298.
[9] F. He, D. Zhao, Preparation and characterization of a new class of starch-stabilized bimetallic nanoparticles for degradation of chlorinated hydrocarbons in water, Environ. Sci. Technol. 39 (2005) 3314–3320.
[10] B. Schrick, B.W. Hydutsky, J.L. Blough, T.E. Mallouk, Delivery vehicles for zerovalent metal nanoparticles in soil and groundwater, Chem. Mater. 16 (2004) 2187–2193.
[11] Y.P. Sun, X.Q. Li, W.X. Zhang, H.P. Wang, A method for the preparation of stable dispersion of zero-valent iron nanoparticles, Colloids Surf. A: Physicochem. Eng. Aspects 308 (2007) 60–66.
[12] F. He, D. Zhao, J. Liu, C.B. Roberts, Stabilization of Fe–Pd nanoparticles with sodium carboxymethyl cellulose for enhanced transport and dechlorination of trichloroethylene in soil and groundwater, Ind. Eng. Chem. Res. 46 (2007) 29–34.
[13] F. He, D. Zhao, Manipulating the size and dispersibility of zerovalent iron nanoparticles by use of carboxymethyl cellulose stabilizers, Environ. Sci. Technol. 41 (2007) 6216–6221.
[14] S.H. Joo, D. Zhao, Destruction of lindane and atrazine using stabilized iron nanoparticles under aerobic and anaerobic conditions: effects of catalysts and stabilizer, Chemosphere 70 (2008) 418–425.
[15] Z. Xiong, D. Zhao, G. Pan, Rapid and complete destruction of perchlorate in water and ion-exchange brine using stabilized zero-valent iron nanoparticles, Water Res. 41 (2007) 3497–3505.
[16] G. Naja, A. Halasz, S. Thiboutot, G. Ampleman, J. Hawari, Degradation of hexahydro-1, 3,5-trinitro-1,3,5-triazine (RDX) using zerovalent iron nanoparticles, Environ. Sci. Technol. 42 (2008) 4364–4370.
[17] Z. Xiong, D. Zhao, G. Pan, Rapid and controlled transformation of nitrate in water and brine by stabilized iron nanoparticles, J. Nanopart. Res. 11 (2009) 807–819.
[18] Q. Wang, H.J. Qian, Y.P. Yang, Z. Zhang, C. Naman, X.H. Xu, Reduction of hexavalent chromium by carboxymethyl cellulose-stabilized zero-valent iron nanoparticles, J. Contam. Hydrol. 114 (2010) 35–42.
[19] F. He, D. Zhao, C. Paul, Field assessment of carboxymethyl cellulose stabilized iron nanoparticles for in situ destruction of chlorinated solvents in source zones, Water Res. 44 (2010) 2360–2370.
[20] J.J. Wei, X.H. Xu, Y. Liu, Kinetics and mechanism of dechlorination of o-chlorophenol by nanoscale Pd/Fe, Chem. Res. Chin. Univ. 20 (2004) 73–76.
[21] S.R. Kanel, D. Nepal, B. Manning, H. Choi, Transport of surface-modified iron nanoparticle in porous media and application to arsenic (III) remediation, J. Nanopart. Res. 9 (2007) 725–735.
[22] E.D. Shchukin, A.V. Pertsov, E.A. Amelina, A.S. Zelenev, Structure, stability and degradation of various lyophobic disperse systems, in: Colloid and surface chemistry, Elsevier Science, Amsterdam, 2001, pp. 629–636.
[23] I.D Morrison, S. Ross, Electrical charges in dispersions, in: Colloidal Dispersions: Suspensions, Emulsions and Foams, Wiley-Interscience, New York, 2002, pp. 316–343.
[24] M. Elimelech, J. Gregory, X. Jia, R.A. Williams, Transport of colloidal materials in groundwater, in: Particle Deposition and Aggregation: Measurement, Modeling and Simulation, Butterworth-Heinemann, Oxford, 1995, pp. 365–368.
[25] R.F. Probstein, Solutions of charged macromolecules and particles, in: Physicochemical Hydrodynamics: An Introduction, 2nd ed., Wiley-Interscience, New York, 1994, pp. 214–223.
[26] W. Stumm, J.J. Morgan, Particle-particle interaction: colloids, coagulation, and filtration, in: Aquatic Chemistry, 3rd ed., John Wiley & Sons, New York, 1996, pp. 834–866.
[27] C.J. Clark, P.S.C. Rao, M.D. Annable, Degradation of perchloroethylene in cosolvent solutions by zero-valent iron, J. Hazard. Mater. 96 (2003) 65–78.
[28] L.J. Matheson, P.G. Tratnyek, Reductive dehalogenation of chlorinated methanes by iron metal, Environ. Sci. Technol. 28 (1994) 2045–2053.
[29] M. Shin, H. Choi, D. Kim, K. Baek, Effect of surfactant on reductive dechlorination of trichloroethylene by zero-valent iron, Desalination 223 (2008) 299–307.
[30] W.A. Arnold, A.L. Roberts, Pathways and kinetics of chlorinated ethylene and chlorinated acetylene reaction with Fe(0) particles, Environ. Sci. Technol. 34 (2000) 1794–1805.
[31] D.R. Burris, T.J. Campbell, V.S. Manoranjan, Sorption of trichloroethylene and tetrachloroethylene in a batch reactive metallic iron–water system, Environ. Sci. Technol. 29 (1995) 2850–2855.
[32] G.N. Jovanovic, P. Plazl, P. Sakrittichai, K. Al-Khaldi, Dechlorination of p-chlorophenol in a microreactor with bimetallic Pd/Fe catalyst, Ind. Eng. Chem. Res. 44 (2005) 5099–5106.
[33] H. Song, E.R. Carraway, Reduction of chlorinated ethanes by nanosized zero-valent iron: kinetics, pathways, and effects of reaction conditions, Environ. Sci. Technol. 39 (2005) 6237–6245.
[34] N. Saleh, K. Sirk, Y.Q. Liu, T. Phenrat, B. Dufour, K. Matyjaszewski, R.D. Tilton, G.V. Lowry, Surface modifications enhance nanoiron transport and NAPL targeting in saturated porous media, Environ. Eng. Sci. 24 (2007) 45–57.
[35] F. He, D. Zhao, Hydrodechlorination of trichloroethene using stabilized Fe–Pd nanoparticles: reaction mechanism and effects of stabilizers, catalysts and reaction conditions, Appl. Catal. B 84 (2008) 533–540.